MOSS LANDING MARINE LABORATORIES

CALIFORNIA STATE UNIVERSITY FRESNO. HAYWARD. SACRAMENTO. SAN FRANCISCO. SAN JOSE STANISLAUS

P O BOx 450
MOSS LANDING CA USA
95039-0450
405 633 3304

AD-A284 841

August 16, 1994

Dr. Edward Green
Office of Naval Research
Oceanic Chemistry Program (Code 323C)
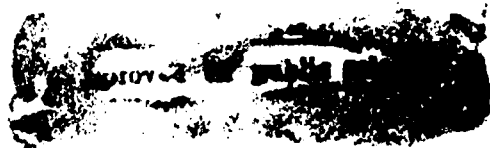800 N Quincy Street
Arlington, VA 22217-5000

Re: Final report for N00014-90-J-4129 Aerosol Iron/Phytoplankton Interactions

Dear Ed,

This is the final report for the Aerosol Iron grant. Under the aegis of this grant two cruises were staged to the equatorial Pacific Ocean in 1990 and 1992. These multidisciplinary cruises were organized by scientists from MLML and Texas A&M to study the role of atmospheric iron inputs in controlling equatorial Pacific ecosystems. Scientists from MLML, Texas A&M, University of Rhode Island, University of Hawaii, MIT and Brookhaven National Laboratories participated in these cruises. Publications from each of these groups have appeared in the literature. A number of conference presentations have been made as well, including a special session at an AGU conference.

The work conducted by MLML scientists has focused on the processes that control Fe bioavailability and its impacts on community level biological processes. Limitation of community growth in the equatorial Pacific was demonstrated by Martin et al. (1991). This work also demonstrated that aerosol iron was biologically available. The role of photochemical reactions in solubilizing this iron was demonstrated by Johnson et al. (1994). Colloidal iron at low nanomolar concentrations was shown to undergo photochemical reduction at a rate sufficient to supply the community with enough monomeric Fe to meet their growth requirements.

Several papers from this cruise are now in preparation. Coale et al. (in prep. for Nature) demonstrate that communities are limited to one half their maximum growth rates at a total iron concentration of 0.12 nM, and they reach saturating growth rates at iron concentrations less than 1 nM. Ambient iron concentrations in the equatorial Pacific are near 0.05 nM and the communities are under severe iron stress. Variations in total iron concentrations across the equatorial Pacific are well correlated with community growth properties, as a result. Fitzwater et al. (in prep. for the Deep-Sea Research EqPac special issue) summarize all of the incubation experiments that have been performed by the Moss Landing group in the equatorial Pacific. The phytoplankton species changes, determined by counting samples, flow cytommetry and by
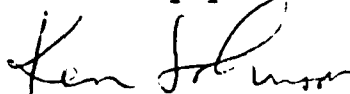
HPLC are addressed in this paper. Gordon et al. (in prep. for the Deep-Sea Research EqPac issue) demonstrate that in the equatorial system inputs of iron driven by equatorial upwelling are the dominant source of iron. These inputs appear to control new primary production in this system.

We are continuing to work on these papers, and expect that they will all by submitted during Fall, 1994. As you are aware, all of the papers from the IronEx cruises have been accepted and will appear in Nature (with a cover photo, we believe) in a few weeks. In addition, a special issue of Deep-Sea Research honoring John Martin and focusing on the IronEx and PlumeEx experiments has been solicited by John Milliman. K. Coale is acting as guest editor for this issue.

Sincerely yours

Kenneth S. Johnson
Professor of Oceanography

Martin, J.H., R.M. Gordon and S.E. Fitzwater. 1991. The case for iron. In: S.W. Chisholm and F.M.M. Morel (eds.): What controls phytoplankton production in nutrient-rich areas of the open sea? ASLO Symposium, Lake San Marcos, California. Feb 22-24, 1991. Limnology and Oceanography, 36, 1793-1802.

Johnson, K. S., K. H. Coale, V. A. Elrod, and N. W. Tindale. 1994. Iron Photochemistry in seawater from the Equatorial Pacific. Marine Chemistry 46, 319-334.

Coale, K. H., S. E. Fitzwater, R. M. Gordon and K. S. Johnson. In prep. Iron limits new production and community growth in the Equatoria Pacific.

Fitzwater, S.E., K. H. Coale, R.M. Gordon, K.S. Johnson and M.E. Ondrusek. In prep. Iron deficiency and phytoplankton growth in the Equatorial Pacific.

Gordon, M., K. Coale and K. Johnson. In prep. Iron distributions in the equatorial Pacific. Implications for new production.

Deep-Sea Research, John Martin Special Issue, Proposed Submissions

Coale, K. H., Fitzwater, S., Blain, S., Coley, T., Hunter, C., K. Johnson, Stanton T., and Watson, A. The design and implementation of a mesoscale iron enrichment experiment in the Equatorial Pacific.

Coale, K. H., Tanner, S., Fitzwater, S. and Hunter, C., Buck, K. and Chavez, F? Phytoplankton species composition and biomass: The partitioning of POC and DOC during the IronEx and PlumEx experiments.

Gordon, M., Coale, K. H. and Johnson, K. S. Trace metal distributions and partitioning during the IronEx and PlumEx experiments in the Equatorial Pacific.

Hoge, F., et al. Distinct Fluorescence Signatures of an Iron-Enriched Phytoplankton Community in the Eastern Equatorial Pacific Ocean.

Hoge, F., et al. Bio-Optics survey of the Galapagos Islands Margins. Airborne chlorophyll, phycoerythrin and DOM fluorescence, upwelled radiance, downwelling irradiance, SST and AXBT profiles.

Kolber, Z., Greene, R., Falkowski, P., et al. Dynamics of photosynthetic response to iron fertilization in the equatorial Pacific.

Greene, R., Kolber, Z., Falkowski, P., et al. Biophysical response of marine phytoplankton to natural iron enrichment as measured by FRR (Fast Repetition Rate) Fluorescence: The PlumEx experiment.

Friederich, G. E., Sakamoto, C. M. and Millero, F. Surface seawater distributions of inorganic carbon and nutrients within the Gaiapagos Plume: Results from the PlumEx experiments using automated chemical mapping.

Stanton, T., et al, Watson, A. et al. The open ocean iron enrichment experiment: Physical evolution of the iron enriched patch.

Watson, A., et al, Millero, F. et al. Evolution of the geochemical signal during the open ocean iron fertilization experiment.

Barber, R., S. Lindley, R. Bidigare, M. Latasa, M. Ondrusek, K. Buck, F. Chavez, S. Chisholm, K. Coale, K. Johnson, S. Tanner, A. Watson, C. Law, K. Van Scoy and M. I. Liddicoat. The In Situ Phytoplankton Response to Natural and Experimental Iron Enrichment.

Lindly S. et al., Changes in the quantum yield of photosynthesis in phytoplankton during the IronEx and PlumEx experiments.

Chisholm et al. The Picoplankton response to iron addition (Plume and Patch and

Bottles).

Chisholm et al. The changes in phytoplankton community size structure (flow cytometrically derive 1 size-fractioned chlorophyll) in iron addition (Plume and Patch and Bottles).

Turner, S. M., Malin, G., Hatton. and Liss, P. S. Iron Fertilization: Effects on dimethyl sulfide and dimethylsulphoniopropionate production.

Nightingale, P. D., Turner, S. M. Malin, G. and Liss, P. S. Iron fertilization: Effects on production of biogenic halocarbons in seawater.

Ondrusek, M., Latasa, M. M., Bidigare, R. Pigment composition and community structure in the IronEx and PlumEx experiments.

Tindale, N. and Seymour, J., and ....? ... osition, concentration and chemical fluxes of atmospheric aerosols during PlumEx. ...si o of single particle analysis.

Collins, C., Steger, J. and G. Montenegro. Upper ocean circulation during the Galapagos Plume experiment: Implications for source waters and mixing.

Chavez, F. et al. Continental shelves, iron fertilization and the structure of phytoplankton communmities.

Lewis, M. R. et al., Bio-optical characteristics of the IronEx experiment and beyond: Results from the optical buoys that would not die. (or: The optical energizer bunny explores the Pacific).

MARINE CHEMISTRY

Iron photochemistry in seawater from the equatorial Pacific

Kenneth S. Johnson[a,b], Kenneth H. Coale[a], Virginia A. Elrod[a], Neil W. Tindale[c]

[a]*Moss Landing Marine Laboratory, PO Box 450, Moss Landing, CA 95039, USA*
[b]*Monterey Bay Aquarium Research Institute, 160 Central Avenue, Pacific Grove, CA 93950, USA*
[c]*Departments of Meteorology and Oceanography, Texas A&M University, College Station, TX 77843, USA*

Iron photochemistry in seawater from the equatorial Pacific

Kenneth S. Johnson[a,b], Kenneth H. Coale[a], Virginia A. Elrod[a], Neil W. Tindale[c]

[a]*Moss Landing Marine Laboratory, PO Box 450, Moss Landing, CA 95039, USA*
[b]*Monterey Bay Aquarium Research Institute, 160 Central Avenue, Pacific Grove, CA 93950, USA*
[c]*Departments of Meteorology and Oceanography, Texas A&M University, College Station, TX 77843, USA*

(Received July 13, 1993; revision accepted February 2, 1994)

Abstract

The photochemistry of iron in surface waters, and its implications to iron bioavailability, was examined on two cruises to the equatorial Pacific. Desktop incubations were performed with equatorial seawater to which iron was added in various chemical forms. Results showed clear diurnal patterns in measurable iron levels, with the highest levels occurring midday. These results are consistent with a model of iron cycling involving the photo-reductive dissolution of colloidal iron and its subsequent oxidation and biological uptake of dissolved iron(III). Model calculations were based on independently determined rate constants. We suggest that photochemical reactions may have a significant impact on iron availability to phytoplankton in the open ocean.

1. Introduction

Iron is thought to be a limiting nutrient that regulates ecosystem structure and primary production in large areas of the ocean (Barber and Chavez, 1991; Coale, 1991; Martin et al., 1991; Martin, 1992). This hypothesis has focused considerable interest on the processes that regulate iron cycling and biological availability in the upper ocean (Wells, 1989; Bruland et al., 1991; Morel et al., 1991). Dissolved iron concentrations in the surface waters of the Pacific are typically < 0.1 nM (Martin, 1992). Iron at this level limits growth in bioassay experiments (Martin et al., 1989, 1991; Coale, 1991). The rate of input of bioavailable iron must exert a strong influence on ocean productivity in these systems. The major source of iron to the remote areas of the world's oceans is deposition of atmospheric dust particles (Donaghey et al., 1991; Duce and Tindale, 1991). However, Wells et al. (1983, 1991a), Finden et al. (1984) and Rich and Morel (1990) have demonstrated that iron oxy-hydroxide particles and iron colloids are not directly available to phytoplankton. Iron particles and colloids must be solubilized to support phytoplankton growth (Rich and Morel, 1990).

Wet deposition of dust particles is typically the major pathway for transport of iron particles to the surface ocean (Duce and Tindale, 1991). Rain squalls can have detectable impacts on the iron concentration in the surface ocean (Hanson et al., 1992). Much of the iron in precipitation may be solubilized within the raindrops by reductive dissolution to Fe(II) driven by the oxidation of SO_2 (Zhuang et al., 1992). However, Fe(II) is oxidized to Fe(III) with a half-life of about 2 min in surface ocean water (Millero et al., 1987). Thus, the reductive dissolution of Fe particles in precipitation may increase the solubility of iron deposited to the ocean, but oxidation and

scavenging onto particles is likely to rapidly transfer the dissolved iron into a biologically unavailable form.

Much work has focused on processes that might solubilize particulate iron in seawater. Production of marine siderophores has been shown to increase iron solubility and bioavailability to some organisms (Trick et al., 1983; Trick, 1989). Recently, Reid et al. (1993) have described a siderophore from a marine bacterium with an exceptionally high ferric ion binding constant, which suggests that siderophores may solubilize iron. However, the presence of siderophores in natural seawater has not been reported and few marine organisms with the capability to produ. · them have been identified (Sunda, 1989; Well., 1989; Bruland et al., 1991).

There has also been considerable interest in the role that photochemical reduction might play in making iron bioavailable (Anderson and Morel, 1982; Finden et al., 1984; Waite and Morel, 1984; Wells and Mayer, 1991; Wells et al., 1991b; Hudson et al., 1992). In this paper, we show that nanomolar concentrations of iron added to equatorial Pacific seawater show a regular, diurnal cycle between a form detected by our analytical method (Elrod et al., 1991), which we presume to be dissolved and bioavailable, and a non-detectable form that is presumably colloidal or particulate iron. The magnitude and timing of this transformation is consistent with a model of photochemical reduction of colloidal and particulate Fe(III). The model represents independent confirmation of our results, as the rate constants are derived from independent studies of iron reactions.

2. Methods

A series of experiments were performed on the FeLINE-I (June 19–July 18, 1990) and FeLINE-II (March 13–April 11, 1992) cruises to the equatorial Pacific. Stations were occupied on a meridional transect across the equator near 140°W. Seawater was collected at a depth where light was approximately 25% of the surface intensity using 30 l Teflon-lined, GoFlo bottles suspended on a Kevlar wire (Martin et al., 1989). This depth was

40 m on FeLINE-I and 25 m on FeLINE-II. The water was added to acid-cleaned, 20 l polycarbonate carboys (Coale, 1991) to which 10 nM iron was added. The iron was added as inorganic iron in the form of $FeNH_4(SO_4)_2$, as organically complexed iron [sodium ferric ethylenediamine di-(o-hydroxyphenyl) acetate] and as natural Asian dust aerosols collected from the remote marine atmosphere. The aerosol sample was collected at the air sampling station on the windward side of Oahu, Hawaii. The trace element composition of this aerosol is dominated by Asian dust (Arimoto et al., 1989). The carboys were then placed in deckboard incubators screened with PVC mesh that reduced the light measured with a PAR meter to 25% of the surface intensity. Surface seawater was circulated through the incubators to maintain constant incubation temperature. Over the course of the incubations samples were collected for the analysis of Fe(III) and Fe(II), nitrate, and chlorophyll.

Iron was determined in samples from the incubators at sea using flow injection analysis with chemiluminescence detection (Elrod et al., 1991). This analytical method is most selective for Fe(II). The sensitivity for Fe(III) is about 5% of that for Fe(II) at temperatures near 20°C. However, we found in this work that the sensitivity to Fe(III) increased dramatically at higher temperatures. At temperatures > 30°C, the signal due to Fe(III) became equal to that for Fe(II). Although this result can be used to develop an effective Fe(III) analysis, it compromised our results for Fe(II) because of the high laboratory temperatures encountered in the ship near the equator (> 23°C on FeLINE-I and in some cases > 30°C on FeLINE-II, due to failure of the ship's air conditioning). We do not report any Fe(II) measurements here, therefore. Iron(III) was determined by reducing sample pH to 5.0 and adding 2 μM of hydroxylamine hydrochloride to the sample for 2 h to reduce dissolved Fe(III) to Fe(II). Samples were filtered (0.45 μm) inline as they were analyzed (Elrod et al., 1991). Thus, the measured iron concentrations are the total reducible iron in solution (TRFe). Detection limits [3 standard deviations (SD) of the blank] were near 0.3 nM.

The sensitivity of the iron analysis to colloidal Fe(III) was determined in the laboratory by analyz-

ing seawater solutions that contained additions of ferrihydrite colloids that were prepared following the procedure of Wells et al. (1991a). A stock solution of 400 μM $FeCl_3$ was allowed to polymerize for 1 h at room temperature. Colloidal ferrihydrite prepared under these conditions is labeled 20°FERR. Colloids with greater degrees of crystallinity were obtained by heating aliquots of the 400 μM stock solution to 50°C (50°FERR) and 90°C (90°FERR) for 5 min. These colloids were then added to seawater at pH 8 to obtain a 10 nM solution, which was kept in the dark at 20°C to prevent photochemical reaction. The TRFe in these solutions was determined as described above.

Nitrate and chlorophyll concentrations in samples from the incubators were also determined at sea. Nitrate was determined as the azo dye (Strickland and Parsons, 1972) using an Alpkem RFA segmented analyzer. Chlorophyll was collected on GF/F glass fiber filters and extracted with 90% acetone for 24 h before analysis with a Turner model 10 fluorometer.

3. Results

3.1 Colloidal iron interference

The concentrations of TRFe observed in the colloidal iron solutions demonstrate that under the conditions of the analysis, as used here, only colloidal iron of very low crystallinity is detected (Fig. 1). Analysis of TRFe in seawater containing colloidal iron always resulted in less than 100% recovery. Experiments reported elsewhere (Coale et al., 1994) have demonstrated that the decrease in iron concentrations is not due to loss of the iron to the carboy walls. The missing iron remains in suspension and can be recovered by acidifying subsamples of the solution to pH = 3.

Only 6.5 ± 0.3 (1 SD) and 0.5 ± 0.1 nM TRFe were detected after 2 h in equatorial seawater (initial iron < 0.3 nM) containing 10 nM of added 20°FERR and 10 nM 90°FERR colloids, respectively. The concentrations of detectable iron dropped to values at or below our detection limits after 24 h in the seawater containing 50°FERR and 90°FERR colloids. This corre-
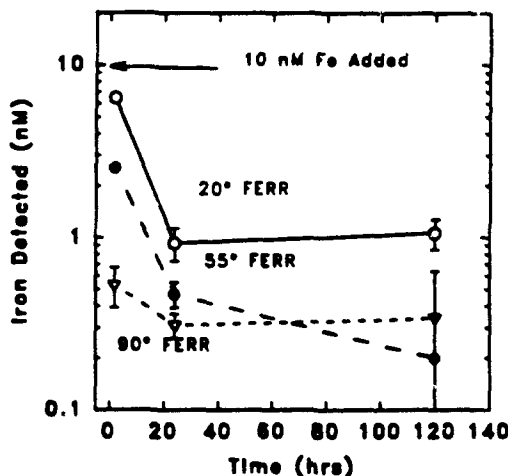

Fig. 1. Total reducible Fe concentrations detected in seawater collected at 15°N, 149°W in 1992 at a depth of 30 m after addition of 10 nM colloidal iron at time zero.

sponds to less than 3% recovery of the heat-treated colloidal iron that had aged 1 day. The concentration of TRFe observed in the seawater containing 10 nM of 20°FERR colloids stabilized near 1 nM within 24 h, or 10% recovery. It is likely that the ferrihydrite formed in our incubation experiments will have a higher degree of crystallinity than the 20°FERR colloids because the rate of formation will be much slower at the low iron concentrations used in our experiments. These results are strong evidence that colloidal iron would be undetectable in our experiments.

3.2 Carboy experiments

Fig. 2 shows the results obtained in 1990 at 3°S, 140°W. The incubation was done using trace metal clean techniques described by Coale (1991). The low growth in the control carboy (+0 Fe) indicates little contamination with iron. Over a period of 5 days, the controls without added iron consumed < 2 μM NO_3^- and chlorophyll increased < 0.5 μg l^{-1}. The carboy with 10 nM Fe added as $FeNH_4(SO_4)_2$ showed complete depletion of nitrate (7 μM NO_3^-) and chlorophyll increased to nearly 4 μg l^{-1} (Fig. 2b). The low growth with no added iron was repeated in replicate control carboys, while a second carboy with 5 nM Fe added as $FeNH_4(SO_4)_2$ showed very similar
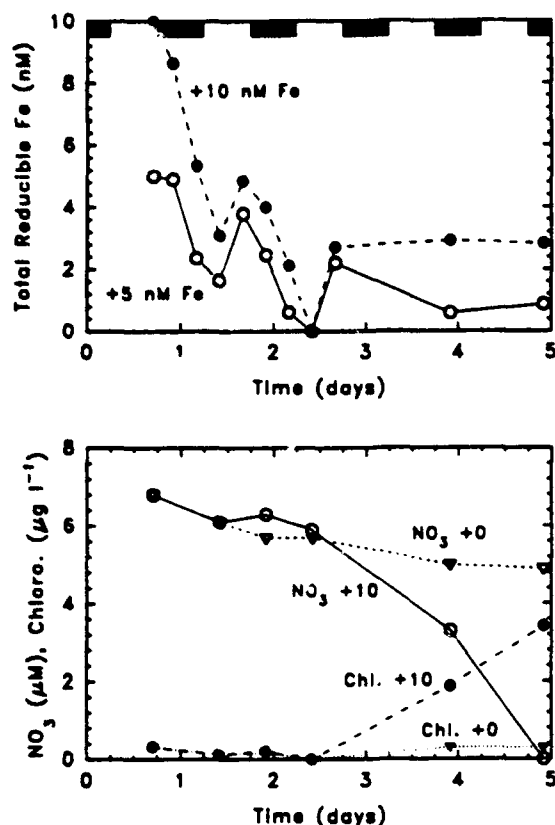
Table 1
Experimental treatments on the 1992 FeLine-II cruise

Carboy	Treatment
1	0.22 μm filtered and 10 nM as FeNH$_4$(SO$_4$)$_2$
2	Control with no added iron
3	10 nM as FeNH$_4$(SO$_4$)$_2$
4	10 nM as FeNH$_4$(SO$_4$)$_2$ + catalase
5	10 nM as sodium ferric ethylenediamine di-(o-hydroxyphenyl) acetate (trade name Sprint 138)
6	≈10 nM Fe as aerosol particles

continued for 2 days with lowest values near dawn and a maximum in late afternoon (Fig. 2a). The amplitude of this cycle was 1–2 nM. Concentrations of iron in carboys without added iron were below our detection limit and the results are not shown.

A second series of incubation experiments was conducted in 1992 near the equator at 140°W. The most detailed study was conducted at a station on the equator (Table 1). At this station, Carboy #1 contained 0.22 μm filtered seawater with 10 nM

Fig. 2. (a) Total reducible Fe concentrations measured over time in carboys with additions of 5 and 10 nM FeNH$_4$(SO$_4$)$_2$. The seawater was collected at 3°S, 140°W in 1990. The light and dark bars indicate day and night. (b) Concentrations of nitrate and chlorophyll measured over time in the carboy with 10 nM Fe(III) added and in a control carboy with no added iron. Concentrations in the carboy with 5 nM Fe(III) added were virtually identical to those measured in the 10 nM addition carboy.

growth and nutrient uptake to that observed in the carboy with +10 nM Fe. Addition of 10 nM Mn, and no Fe, to a carboy without added iron did not produce extra growth (not shown).

The additions of +10 and +5 nM Fe(III) in these incubations were made at sunset. The concentration of TRFe decreased rapidly in the carboys during the 12 h dark period that followed to a low of 3.1 nM in the +10 carboy and 1.7 nM in the +5 carboy (Fig. 2a). Concentrations of TRFe began to increase after sunrise and reached maximum values of 4.8 and 3.8 nM TRFe in the afternoon. A distinct diurnal cycle in the TRFe concentration
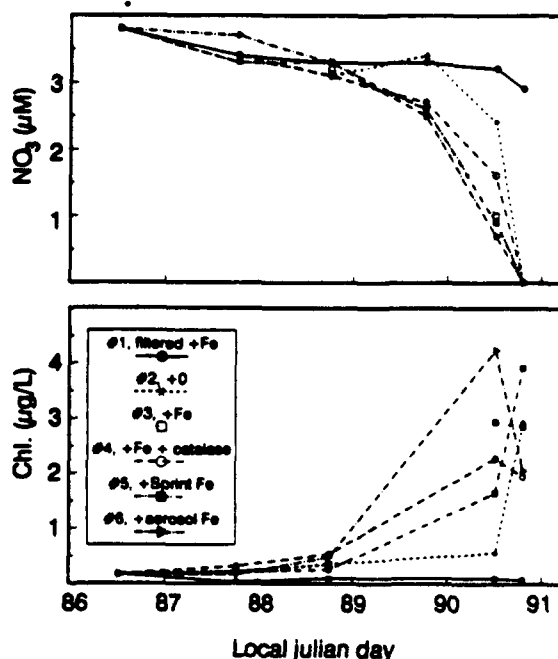

Fig. 3. Nitrate and chlorophyll concentrations, respectively, measured over time in carboys containing seawater collected at 0°N, 140°W in June, 1990.

Fe(III) added as $FeNH_4(SO_4)_2$ and, as expected, showed no increase in chlorophyll or depletion in nitrate (Fig. 3). Carboys #3–#6 in this experiment all contained ca. 10 nM iron added in various forms (Table 1). The chlorophyll increased and nitrate was depleted in all 4 of these carboys. The carboy with iron added as aerosol particles (#6) showed the most rapid growth and attained the highest chlorophyll levels (Fig. 3). Carboy #5 with organically complexed iron also showed relatively high growth compared to the carboys with inorganic iron (#3 and #4). The control in carboy #2 without added Fe did grow, but it always lagged behind the other treatments. It has been suggested that atmospheric inputs of iron were high during the spring of 1992 due to enhanced atmospheric inputs that resulted from the El Nino conditions and the Mt. Pinatubo eruption. The control incubations performed during the spring of 1992 in the equatorial Pacific by J. Martin's research group also showed relatively high growth (J. Martin and S. Fitzwater, pers. commun., 1993), which suggests unusually high Fe levels.

Fig. 4 shows the iron data from these experiments. Total reducible iron concentrations in Carboy #1 showed a large change on the first day (amplitude $\approx$ 2 nM) and then a much attenuated cycle (amplitude < 1 nM) over the remainder of the experiment when compared to its unfiltered companion experiment in Carboy #3. The TRFe concentrations in Carboy #3 underwent a pronounced diurnal cycle over the complete experiment with an initial amplitude of 2 nM that gradually decreased to about 1 nM as concentrations dropped over the 4 day experiment. Addition of catalase to Carboy #4, to suppress the H_2O_2 concentration, had relatively little impact on iron concentrations (Fig. 4). Similar diurnal cycles were seen in Carboy #5 with the Sprint-138 complex and in Carboy #6 with aerosol iron. However, the mean level of TRFe was much lower in these two carboys than in the carboys to which $FeNH_4(SO_4)_2$ was added. Iron concentrations in the control carboy (#2) remained below our detection limit for the experiment.

A second incubation experiment was performed at 15°N, 149°W. There was very little nitrate in surface water at this station (< 0.1 μM NO_3^-) and
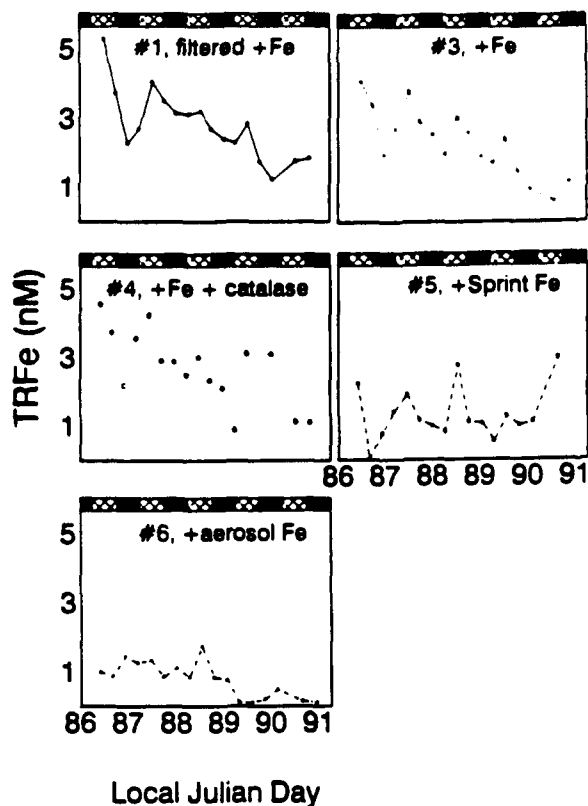

Fig. 4. Total reducible Fe concentrations detected in the carboy experiments at 0°N, 140°W in 1992. The treatments of each carboy are described in Table 1. No iron was detected at concentrations above our detection limits in Carboy #2 and the results for that experiment are not shown. The light and dark bars indicate day and night.

there was no growth in any of the carboys. Data for chlorophyll and nitrate in these experiments are not shown, therefore. Fig. 5 shows the TRFe data from the experiment at 15°N. The TRFe concentrations again show a distinct diurnal periodicity. There were no detectable differences among the various treatments, which were the same as at the equatorial statio : (Table 1).

Phytoplankton were able to grow with all of the different chemical forms of iron that were added to the incubation experiments performed at the equator in 1992 (Fig. 3). Particulate iron, in the form of aerosol particles was one of the most efficient producers of chlorophyll, which is a good proxy for biomass in these experiments (Martin et al., 1991). Chelated iron also produced high chlorophyll
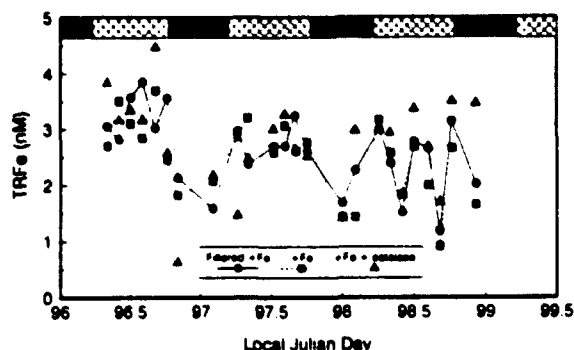
Fig. 5. Total reducible Fe concentrations detected in a carboy experiment at 15°N, 149°W in 1992. Treatments in each carboy are the same as those described in Table 1. The light and dark bars indicate day and night

levels. Some process must be converting the iron to a dissolved chemical form that is available to the plankton, as laboratory experiments demonstrate that organically bound iron (Anderson and Morel, 1982) and colloidal iron (Rich and Morel, 1990) are not directly bioavailable. The diurnal cycle in TRFe concentration suggests that this process involves a photochemical step. We have, therefore, examined the available data on iron photochemistry in seawater to ascertain whether or not a photochemical cycle is consistent with our results.

3.3 Photochemical model

The diurnal cycles of iron that were observed in the incubation experiments would require the existence of a minimum of three photolabile iron species: a soluble Fe(III) species that is detected by the FIA-CL analysis, an undetectable Fe(III) species that we assume to be colloidal, and Fe(II) that is the product of a photochemical reduction reaction. It is also possible that the undetectable iron is bound to particles or an organic ligand. Some role for particulate iron in the photochemical cycle is suggested by the differences between the diurnal cycles of iron observed in filtered (Carboy #1) and unfiltered (Carboy #3) seawater at the equatorial station in 1992 (Fig. 4). There is no evidence for strong complexation of nanomolar levels of iron in seawater (Bruland et al., 1991). For simplicity, we have modeled the

undetectable iron species as a single species, which we call FeC. The FeC may, in fact, be colloidal, particulate or organically complexed Our analytical protocol would not detect any of these forms of iron.

Fig. 6 shows a schematic of a model that we have used to simulate the photochemical cycle of iron. It is based upon the minimum set of three iron species and it is similar to that developed by Anderson and Morel (1982) and by Hudson and Morel (1990) The three iron species undergo a total of 6 reactions. Dissolved Fe(III) forms colloids (step A). The colloidal FeC is then photoreduced via step B. Dissolved Fe(III) can also be photoreduced directly (step C). The Fe(II) is then reoxidized to Fe(III) by oxygen (step D) or by hydrogen peroxide (step E). The Fe(III) is also incorporated into cells. where it is essentially removed from the system (step F). Hydrogen peroxide also decays (step G).
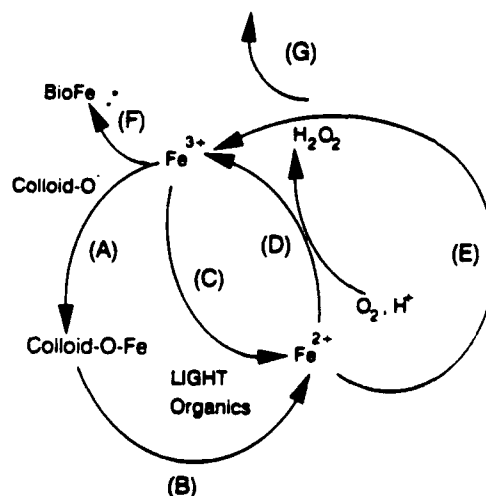
The rate constants for each of the steps in the model were all adapted from the literature or

Fig. 6. Schematic of the reactions used to model the photochemical cycle of iron. Dissolved, monomeric Fe^{3+} species [including $Fe(OH)_n^{3-n}$] react via step A to form colloidal Fe(III) species. Colloidal Fe(III) species are photoreduced via step B Dissolved, monomeric Fe^{3+} is also photoreduced directly via step C. Dissolved Fe^{2+} produced via the photoreduction reactions is oxidized back to dissolved, monomeric Fe^{3+} by reaction with oxygen (step D) or by reaction with hydrogen peroxide (step E). Dissolved, monomeric Fe^{3+} is also incorporated into biomass via step F. Finally, we have included a decay reaction for the hydrogen peroxide produced from superoxide ions (step G)

periments at sea. The rate constant for formation ˙ colloidal iron (step *A*) was determined by measuring the change in dissolved Fe(III) concentrations during dark periods after the addition of re initial 10 nM Fe(III) spike (e.g. Fig. 2). A plot f concentration vs. time during the initial dark eriod is linear on a semi-log plot, indicating rst-order kinetics with a rate constant $k_C = 0.1$ $^{-1}$ (Fig. 7). The rate law for step *A* is:

$$\frac{\partial [Fe(III)]}{\partial t} = -k_C[Fe(III)] \tag{1}$$

he photoreduction rate constant of colloidal iron nd that for dissolved iron were calculated from the oeasurements in coastal seawater at pH 6.5 by Waite and Morel (1984). They added Fe as an amorphous FeOOH stock solution to filtered, coastal seawater and found a photoreduction rate of 14 nmol Fe(II) $(\mu mol\ FeOOH)^{-1}\ min^{-1}$ at an irradiance of 30 $\mu E\ ml^{-1}\ min^{-1}$ from a solar simulator and a pH of 6.5. We assume that this photoreduction rate applies to the FeC species and that the reaction is first order with respect to FeC concentration. An irradiance of 30 $\mu E\ ml^{-1}\ min^{-1}$ is a typical value at noontime in the equatorial Pacific. We assume that this is the maximum rate possible.

Fig 7. Total reducible Fe concentrations measured in the first 12 h dark period after addition of 5 and 10 nM FeNH₄(SO₄)₂ to seawater. The lines for each experiment correspond to first-order removal rates of 0.10 h⁻¹. Time zero data points are the calculated initial concentration and were not directly measured. These results correspond to the first 3 data points in Fig. 3 (top).

and the photoreduction rate decreases linearly with the irradiance. The rate law for photoreduction of colloidal Fe(III) is (step *B*):

$$\frac{\partial [Fe(II)]}{\partial t} = -\frac{\partial [Fe(III)]}{\partial t} = \frac{k_{h\nu C}[FeC]I}{I_0} \tag{2}$$

where [FeC] is the concentration of the undetectable, colloidal iron species, *I* is the irradiance and $I_0 = 30$ $\mu E\ ml^{-1}\ min^{-1}$. The rate constant $k_{h\nu C} = 0.84$ h^{-1}. This equation assumes the reaction is proportional only to the solar flux, and it ignores the wavelength dependence of the reaction. Rich and Morel (1990) have shown that only light at wavelengths less than 560 nm can photoreduce iron. Wells et al. (1991b) have shown that only light at wavelengths less than 400 nm reduces ferrihydridite present at relatively high (4 μM) concentrations. However, there are few other data available regarding the spectral dependence of the reaction and we are forced to make this simplification.

Waite and Morel (1984) concluded that photoreduction was much slower at pH 8 because no Fe(II) accumulated in their experiments at pH 8. However, their results are also consistent with a pH independent rate of photoreduction and a much higher rate of Fe(II) oxidation at pH 8 that would keep Fe(II) concentrations below their detection limits (Hudson et al., 1992). Hudson et al. (1992) recently performed an experiment to check this hypothesis by adding an organic ligand to seawater to trap any Fe(II) formed by photoreduction and prevent its reoxidation to Fe(III). They found that about 30% of the ferric hydroxide colloids precipitated in a solution containing humic acids were photoreduced in 1 h after the colloids were added to synthetic seawater at pH = 8. This corresponds to a rate constant of 0.3 h^{-1} at pH = 8, in relatively good agreement with the value that we derived from Waite and Morel (1984). This agreement suggests that there is not a strong pH dependence of photoreduction rates between pH 6.5 and 8. Wells and Mayer (1991) also examined the photoconversion of ferrihydrite to labile forms that could be extracted from seawater by complexation with oxine. Photoreduction rates derived from their work are about 10–50-fold lower than the values that we used. This may result because they used high concentrations
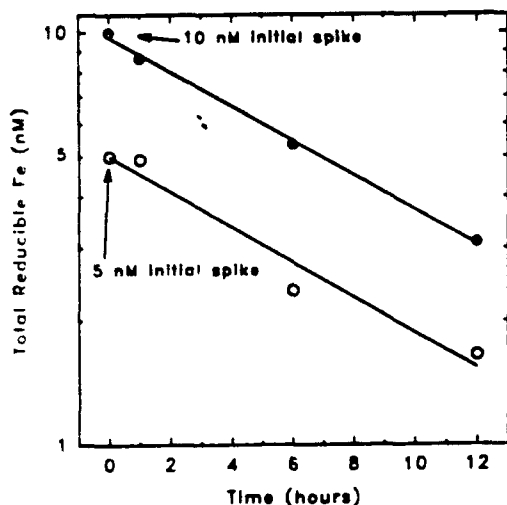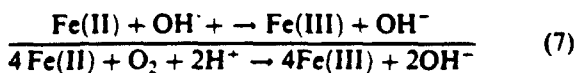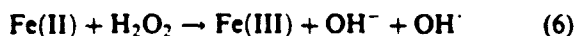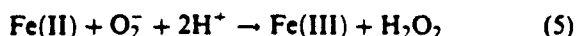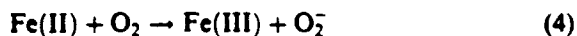
of ferrihydrite colloids (1-5 μM) that exceeded the concentration of chromophores present in solution, or because some of the photoreduced iron reoxidizes to iron species that are unavailable to their analytical method during the photolysis experiment. We assume that the results of Waite and Morel (1984) also apply at pH 8.

The photoreduction rate of dissolved Fe(III) was also determined from the measurements of Waite and Morel (1984). In their experiments, additions of 42 and 84 nM Fe(III) as an FeCl$_3$ solution to filtered coastal seawater at pH = 6.5 produced 9 and 14.5 nM Fe(II) after 2 h of irradiation at 30 μE ml^{-1} min^{-1} with a solar simulator. After correcting their results for the production of Fe(II) in seawater with no added iron (4.4 nM per 2 h irradiation), and assuming first-order reaction kinetics that are pH independent, we calculate the rate law for photoreduction of dissolved Fe(III) (step C) to be:

$$\frac{\partial[\text{Fe(II)}]}{\partial t} = -\frac{\partial[\text{Fe(III)}]}{\partial t} = \frac{k_{h\nu D}[\text{Fe(III)}]I}{I_0} \qquad (3)$$

where $k_{h\nu D} = 0.055$ h^{-1}. This rate constant presumably represents the photoreduction rate of dissolved Fe^{3+} before colloids have formed in solution.

Rate constants for the oxidation of Fe(II) are also required in this model. The oxidation of Fe(II) by reaction with oxygen (step D) is believed to proceed via the Haber-Weiss mechanism (Stumm and Morgan, 1981):

$$\text{Fe(II)} + \text{O}_2 \rightarrow \text{Fe(III)} + \text{O}_2^- \qquad (4)$$

$$\text{Fe(II)} + \text{O}_2^- + 2\text{H}^+ \rightarrow \text{Fe(III)} + \text{H}_2\text{O}_2 \qquad (5)$$

$$\text{Fe(II)} + \text{H}_2\text{O}_2 \rightarrow \text{Fe(III)} + \text{OH}^- + \text{OH}^\cdot \qquad (6)$$

$$\frac{\text{Fe(II)} + \text{OH}^\cdot + \rightarrow \text{Fe(III)} + \text{OH}^-}{4\,\text{Fe(II)} + \text{O}_2 + 2\text{H}^+ \rightarrow 4\text{Fe(III)} + 2\text{OH}^-} \qquad (7)$$

Moffet and Zika (1987) have concluded that this pathway is unlikely to go to completion at the low metal concentrations found in seawater because many of the radicals involved in reactions (5)-(7) will be scavenged by other processes. We have considered each of these reactions separately in the model, therefore.

Millero et al. (1987) measured the rate of reaction of Fe(II) with O$_2$ in seawater. These measurements were made at micromolar iron concentrations. High Fe(II) concentrations favor the completion of the entire mechanism rather than loss of the radicals by other pathways. Their results correspond to the sum of reactions (4)-(7). Reaction (4) is believed to be the rate limiting step in the chain. The rate constant for reaction (4) (k_{O_2}) can be obtained by reducing the rate constants reported by Millero et al. (1987) by 1/4, therefore (Moffet and Zika, 1987). The rate law for step D of the model is (Millero et al., 1987):

$$\frac{\partial[\text{Fe(II)}]}{\partial t} = -k_{O_2}[\text{Fe(II)}][\text{O}_2][\text{OH}^-]^2 \qquad (8)$$

Millero and Sotolongo (1989) measured the rate of reaction of Fe(II) with H$_2$O$_2$ in seawater, again at high iron concentrations which favored completion of reactions (6) and (7). Reaction (6) is the slowest of these two steps (Moffet and Zika, 1987). The rate constant for reaction (6) ($k_{H_2O_2}$) is obtained by reducing the rate constant reported by Millero and Sotolongo (1989) by 1/2. The rate law for step E of the model is (Millero and Sotolongo, 1989):

$$\frac{\partial[\text{Fe(II)}]}{\partial t} = -k_{H_2O_2}[\text{Fe(II)}][\text{H}_2\text{O}_2][\text{OH}^-] \qquad (9)$$

The values of k_{O_2} and $k_{H_2O_2}$ used in the model were calculated from the equations reported by Millero et al. (1987) and Millero and Sotolongo (1989) at the appropriate temperature, salinity, pH (free proton scale) and oxygen concentration for each numerical experiment and corrected for stoichiometry as discussed here. The pseudo first-order rate constants calculated from Millero's work at pH = 8.2, 25°C, salinity = 35 (Practical Salinity Scale), oxygen = 214 μM (100% saturation), and 50 nM H$_2$O$_2$ were $k'_{O_2} = 21$ h^{-1} and $k'_{H_2O_2} = 13$ h^{-1}. Hydroxide ion concentrations were calculated from the pH using the dissociation constant of water in seawater (Millero et al., 1987). The value of $k'_{H_2O_2}$ was recalculated at each time step as the concentration of H$_2$O$_2$ changed over the course of a simulation.

No measurements of the rates of reactions (5) or (7) in seawater are available. However, the radicals involved in these reactions are likely to be consumed by a variety of other reactions in seawater when dissolved Fe(II) concentrations are low (Moffett and Zika, 1987). For example, 60-80% of the superoxide ion formed in seawater disproportionates to form H_2O_2 (Petasne and Zika, 1987) and would not be available to oxidize Fe(II). The hydroxyl radical formed in reaction (6) is also likely to react by other pathways. Mopper and Zhou (1990) estimated that reaction with Br^- scavenges 93% of the OH· formed in seawater. We have assumed, in the absence of any additional quantitative data which could be used in the model, that all of the superoxide ion disproportionates to form H_2O_2 and that all of the hydroxyl radical is scavenged by other reactions. The rates of reactions (5) and (7) are negligible in this scenario and they are not included in the model. Incorporation of these reactions has no discernable effects except on Fe(II), as discussed below.

A simplified scheme for H_2O_2 cycling was incorporated into the calculations to assess the effect that iron photochemistry could have on diurnal cycling of hydrogen peroxide. Assuming that all of the superoxide disproportionates to H_2O_2 and O_2, the rate of formation of H_2O_2 is 1/2 of the rate at which Fe(II) is oxidized by oxygen in this case. One molecule of H_2O_2 is also lost each time it reacts with Fe(II). The rate of this reaction was estimated from the rate law determined by Millero and Sotolongo (1989). A first-order term for decay of hydrogen peroxide was also incorporated. Plane et al. (1987) report a decay time for H_2O_2 of 4 days, which corresponds to a first-order rate constant of $k_d = 0.01$ h^{-1}. Similar results have been observed by Johnson et al. (1989). No other terms for H_2O_2 production or consumption were included.

Finally, a term was incorporated into the model to account for biological uptake of iron as biomass increased during the experiments. The uptake was assumed to be first order in Fe(III). The rate constant was estimated from the increase in chlorophyll observed over the course of the incubations, the C:chlorophyll ratio in plankton (Chavez et al., 1991), and the Fe:C ratio in plankton from oligo-

trophic systems (Morel et al., 1991). This gave a value $k_{bio} = 0.02$ h^{-1}.

The overall rate laws governing the production of dissolved Fe(III), Fe(II) and particulate Fe(III) (FeC) are then:

$$\frac{\partial[Fe(III)]}{\partial t} = -k_{h\nu D}[Fe(III)]\frac{I}{I_0} - k_C[Fe(III)]$$
$$+ k_{O_2}[Fe(II)][O_2][OH^-]^2$$
$$+ k_{H_2O_2}[Fe(II)][H_2O_2][OH^-]$$
$$- k_{bio}[Fe(III)] \qquad (10)$$

$$\frac{\partial[Fe(II)]}{\partial t} = k_{h\nu D}[Fe(III)]\frac{I}{I_0} + k_{h\nu C}[FeC]\frac{I}{I_0}$$
$$- k_{O_2}[Fe(II)][O_2][OH^-]^2$$
$$- k_{H_2O_2}[Fe(II)][H_2O_2][OH^-] \qquad (11)$$

$$\frac{\partial[FeC]}{\partial t} = k_C[Fe(III)] - k_{h\nu C}[FeC]\frac{I}{I_0} \qquad (12)$$

The equation governing hydrogen peroxide production and decay is:

$$\frac{\partial[H_2O_2]}{\partial t} = 0.5k_{O_2}[Fe(II)][O_2][OH^-]^2$$
$$- k_{H_2O_2}[Fe(II)][H_2O_2][OH^-]$$
$$- k_d[H_2O_2] \qquad (13)$$

The light intensity (I/I_0) in the model was generated by using a cosine function to vary irradiance (I) from 0 to I_{max} and back to 0 over a 12 h period, followed by a 12 h dark cycle. The initial concentrations of hydrogen peroxide were set to 25 nM, which is similar to the values observed in the surface water and in the carboys (W. King, pers. commun., 1990). The concentrations of Fe(II), Fe(III), FeC and H_2O_2 were then obtained by integrating the equations numerically by finite differences using Euler's method. All calculations were performed using iterative calculations and macro commands in a LOTUS 1-2-3 spreadsheet program. Simulation of a 24 h cycle required only 40 s on a 50 Mhz 80486 IBM compatible computer. The accuracy of the results was checked by reducing the time step from 0.002 to 0.0001 h for a subset of the calculations and verifying that the same solutions were obtained. The sensitivity of the

model results to the various rate constants is discussed below.

Fig. 8 shows results of a model run for pH 8.2 seawater with I_{max} set equal to $0.25 \times I_0$, where I_0 is the noontime solar irradiance at the sea surface, which we assume to produce 30 μE cm^{-3} min^{-1}. This is approximately equal to a solar flux of 1000 W m^{-2} at the sea surface. The model results for dissolved Fe(III) are in excellent agreement with the observed TRFe concentrations observed in the carboy experiments. The modeled concentrations of Fe(III) show a diurnal concentration change of about 3 nM, which is slightly larger than the observed changes in TRFe concentration. This change is diurnal cycle is driven by the formation of colloidal Fe(III) and its subsequent photoreduction. As iron is consumed by phytoplankton, the overall level of iron in the system decreases and the amplitude of the modeled photochemical signal decreases at about the same rates as observed in Carboy #3.

One adjustment was made to the model parameters to produce the agreement shown in Fig. 8. The amount of added iron in the model was set equal to 7 nM, rather than the 10 nM addition
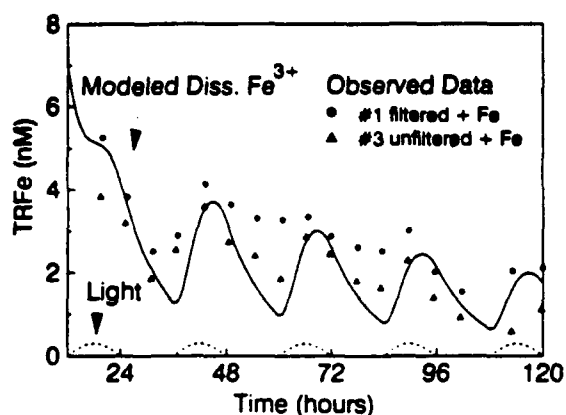

Fig. 8. The solid line shows the concentration of dissolved, monomeric Fe^{3+} predicted with the numerical model after the addition of 7 nM Fe^{3+} to seawater. The dashed line shows the light intensity cycle (I/I_0) used to drive the photochemical cycles. Maximum values of I/I_0 were 0.25, which corresponds to a depth of 25 m. For comparison, the concentrations of total reducible Fe measured in carboys shielded with PVC netting to reduce light to 25% of the surface intensity are also shown. Iron was added to a concentration of 10 nM in each carboy. Carboy #1 was 0.22 μm filtered, while carboy #3 was unfiltered.

used in the carboy experiment. Without this adjustment, the model results are 3 nM higher than the observed values. This offset may represent the loss of a portion of the iron added to the carboys into a non-photolabile form, or it may represent rapid luxury uptake of iron by phytoplankton. Similar losses of iron were observed in the subarctic Pacific (Coale, 1991).

Filtration of the seawater might be expected to reduce photoreduction rates if the reaction occurs primarily on surfaces. The diurnal cycle of TRFe was much attenuated in Carboy #1 (0.22 μm filtered to remove phytoplankton) after the first day in the 1992 experiment, when compared to the model results or the results observed in Carboy #3 (Fig. 8). However, photoreduction rates were high in Carboy #1 on the first day and the amplitude did not decrease until the second day. Surfaces of filterable particles do not seem to play an important role in the photoreduction reaction, therefore. One possible explanation for the reduced photoreduction rate on day 2 is that phytoplankton produce a short-lived, dissolved compound that promotes photoreduction. Enough of this compound would have to remain in solution after filtration to allow photoreduction to occur on the first day but not on subsequent days. However, in the absence of replicate experiments on filtered carboys at the equator, these conclusions must remain tentative.

The amplitude of the diurnal change in iron concentration is similar in both the filtered and unfiltered carboys at the $15°N$ station during 1992 (Fig. 5). The low nitrate concentrations (< 0.1 μM) at this station supported a very low biomass (chlorophyll$\approx$0.05 μg l^{-1}). This may account for the lack of difference between filtered and unfiltered experiments.

The sensitivity of the model predictions of dissolved Fe^{3+} concentrations to changes in the rate constants is shown in Fig. 9. A baseline run of the model predicted concentrations of dissolved Fe(III) is plotted in this figure. These values were calculated using the rate constants discussed above. Model runs were also made with the following changes from the baseline case: a two-fold reduction in $k_{h\nu C}$, $k_{h\nu D}$ set to zero, a two-fold reduction in the colloid formation rate constant
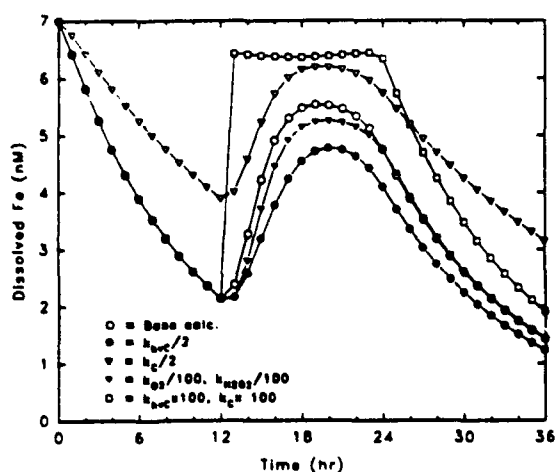
Fig. 9. The effect of changing the reaction rate constants on predicted concentrations of dissolved Fe^{3+}. The base calculation (O) uses the rate constants discussed in the text. These are the same as in Fig. 8. except that the model run begins at the start of the dark period. The predicted concentrations obtained for a two-fold decrease in the photoreduction rate of colloidal iron (●), and a two-fold decrease in the rate of formation of colloidal iron (▽) are shown. A 100-fold decrease in the oxidation rates of Fe^{2-} by oxygen and hydrogen peroxide (▼), which simulates complexation of 99% of the Fe^{2-} by a strong ligand, is also shown. Finally, a scenario with 100-fold increases in the photoreduction rate of colloidal iron and rate of formation of colloidal iron (□) is shown.

k_C. a 100-fold decrease in both k_{O_2} and $k_{H_2O_2}$, and a 100-fold increase in both photoreduction rate constants (Fig. 9).

The rate constants that have the greatest effect upon the diel change in Fe(III) concentrations are the photoreduction rate of colloidal iron ($k_{h\nu C}$) and the rate of formation of colloidal iron (k_C). Setting $k_{h\nu D}$ to zero has no effect on the Fe(III) concentrations. Photoreduction of dissolved Fe(III) is negligible compared to photoreduction of the colloidal Fe(III) and only very large increases in its rate constant will have an effect on model output. A 50% reduction in $k_{h\nu C}$ reduces the amplitude of the diurnal cycle of Fe(III) by only 25%. The non-linear relationship between a change in $k_{h\nu C}$ and the amplitude of the Fe(III) diurnal cycle is produced by the first-order kinetics used for formation of colloidal Fe(III) and photoreduction of colloidal Fe. The two-fold reduction in colloid formation rate increases the minimum

Fe(III) concentration by nearly a factor of two and the amplitude of the diurnal change is reduced by about 30%. Large changes in the oxidation rate of Fe(II) have almost no effect on the Fe(III) concentration predicted with the model. For example, there is no discernable change in any of the Fe(III) species if all of the radicals produced during Fe(II) oxidation react completely with Fe(II). The results are not sensitive to the oxidation rate because it is so fast compared to photoreduction or colloid formation rates that the Fe(II) pool is negligible in size compared to the Fe(III) pool.

The maximum Fe(II) concentrations that are obtained in the baseline model calculation are 0.033 nM. The steady state concentration of Fe(II) predicted from Eq. (11) at maximum irradiance (I_0) is:

$$[Fe(II)]_{ss} = \frac{k_{h\nu C}[FeC]}{k'_{O_2} + k'_{H_2O_2}} = 0.017[FeC] \qquad (14)$$

if the slow photoreduction step for dissolved Fe(III) is ignored. This steady state equation predicts maximum concentrations of Fe(II) that are only 0.5% of the total iron concentration.

Substantial (> 10% of dissolved iron) Fe(II) concentrations can only be supported by 30-fold decreases in the Fe(II) oxidation rate or by a combined increase in the photoreduction rate and colloid formation rate. A 100-fold decrease in the Fe(II) oxidation rates would produce maximum Fe(II) concentrations of about 0.5 nM with total iron concentrations of 7 nM (Fig. 9). A 100-fold increase in both of the photoreduction rates will produce Fe(II) concentrations of only 0.1 nM because photoreduction rapidly transfers iron from the colloidal reservoir with high photoreduction rates to the dissolved Fe(III) pool where photoreduction rates are low with even a 100-fold increase. An increase in photoreduction rates must be accompanied by an increase in the rate of colloid formation to maintain high Fe(II) concentrations.

Hydrogen peroxide is generated in the model by disproportionation of the superoxide ion produced by reaction of oxygen with Fe(II). The predicted concentration of H_2O_2 shows a diurnal cycle with an amplitude of about 2 nM in simulations with

25% of the surface light intensity and 7 nM added iron. Maximum concentrations occur at local noon. In comparison, diurnal cycles of hydrogen peroxide observed in the Gulf of Mexico are much larger, with an amplitude of about 25 nM (Zika et al., 1985). The amount of hydrogen peroxide produced by photochemical cycling of iron in oligotrophic waters will be much less because concentrations of photolabile iron are 100 times lower than were used in the simulation. Thus, redox cycling of iron is unlikely to produce significant amounts of hydrogen peroxide.

Hydrogen peroxide concentrations also seemed to have little direct effect on the photocycling of iron. The TRFe levels in carboys to which catalase had been added were not substantially different than similar experiments without catalase (Figs. 4 and 5). The effects of adding catalase to a carboy were also simulated with the model by increasing the decay rate of hydrogen peroxide (k_d) by a factor of 100. The hydrogen peroxide concentrations remained below 0.7 nM in this simulation. The iron concentrations changed by less than 0.001 nM, relative to the baseline model calculation.

4. Discussion

The results presented here are strong evidence for the existence of an active iron photochemical cycle in surface seawater. The observations made in carboy experiments show distinct diurnal cycles in iron concentrations. These observations are supported by a model derived from independently published measurements.

How will photochemical reactions affect the distribution of dissolved iron in surface waters? To answer this question, we have used the numerical model to simulate the diurnal cycle of iron in equatorial waters using the measurements of filterable and particulate iron in the euphotic zone at $0°N$, $140°W$ that were reported by Martin (1992). Concentrations of iron that pass through a 0.45 μm filter averaged 0.05 nM in the upper 100 m and particulate iron averaged 0.2 nM. It is likely that much of the particulate Fe is refractory and not reducible. We estimated the refractory Fe concentration to be 0.1 nM, based on the particulate aluminum concentration observed by Martin (1992) (0.2 nM) and the Fe:Al ratio in crustal rock (3 mol Al:mol Fe). The pool of photolabile Fe (dissolved + reducible colloidal + reducible
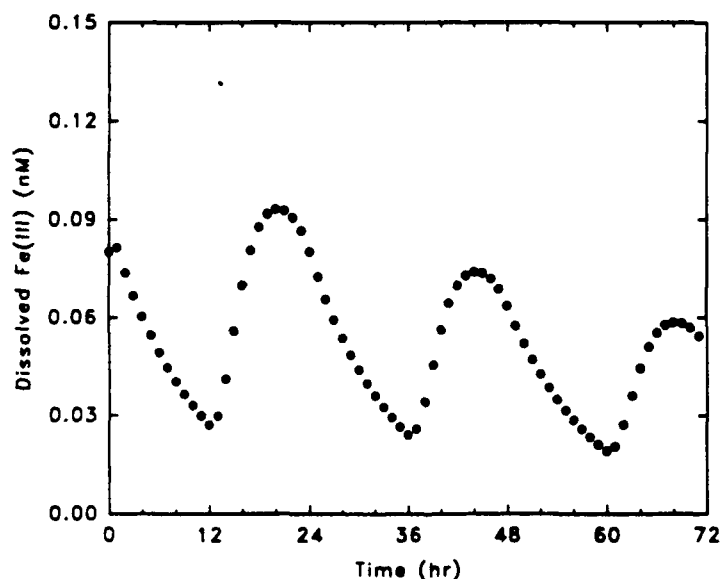

Fig. 10. The simulated concentration of dissolved, monomeric Fe^{3-} is shown for a system with a total concentration of photolabile Fe equal to 0.15 nM, similar to that expected for surface waters in the equatorial Pacific. The maximum light intensity was 0.5 I_0, corresponding to a depth near 10 m.

particulate) was set equal to 0.15 nM Fe, therefore.

The diurnal cycle of iron that results in seawater containing 0.15 nM of photolabile iron that has a photoreduction rate similar to colloidal iron is shown in Fig. 10. The particulate and colloidal pool of iron is rapidly photoreduced and dissolved concentrations that vary within the concentration range 0.03–0.09 nM are produced. These dissolved iron concentrations bracket the range of filterable iron concentrations observed by Martin (1992). However, it is difficult to compare the results of the model developed here with conventional measurements of dissolved and particulate iron distributions in the sea. Dissolved iron is usually determined as the total amount of iron in samples that have been passed through a 0 45 μm filter and then acidified to a pH near 2. This fraction will contain both the truly dissolved iron and the colloidal iron. We refer to this fraction as filterable iron to distinguish it from dissolved iron. No diurnal cycles would be observed in the concentration of filterable iron if colloidal iron was the main product of reaction (A).

In the oligotrophic waters of the central North Pacific, conventional measurements of filterable iron follow a nutrient like profile with concentrations that rise from < 0.1 nM near the surface to values of 0.7 nM at 2000 m depth (Martin and Gordon, 1988; Martin et al., 1989). If photochemical reactions are required to produce dissolved iron, then much of the filterable iron must be colloidal material. This suggests that the solubility of iron is much less than 1 nM. There is considerable uncertainty regarding the solubility of dissolved iron in seawater. Byrne and Kester (1976) suggested that dissolved iron concentrations as high 20 nM could be found in pH 8 seawater. However, this result has been questioned by Zafiriou and True (1980). They suggest a much lower solubility for Fe(III) at pH 8. Zhu et al. (1992) have also reanalyzed the data of Byrne and Kester (1976) and obtained an Fe(III) solubility of 0.6 nM at pH 8. Recently, Hudson et al. (1992) have also concluded that their experimental results are consistent with a solubility of Fe(III) that is <1 nM at pH 8. Motekaitis and Martell (1987) have calculated a solubility for

Fe(III) in seawater of 0.1 nM. As colloids age. the solubility may drop even further. Thus, it is possible that a high percentage of the iron in seawater, which passes through a 0.45 μm filter. is colloidal, even at total iron concentrations < 1 nM.

Manganese is an element that also undergoes an active photoreduction cycle in seawater (Sunda and Huntsman, 1988). Manganese photoreduction is believed to contribute to the formation of the near-surface concentration maximum that is often observed in vertical profiles of dissolved Mn concentrations (Sunda and Huntsman, 1988). Near-surface concentration maxima in dissolved iron concentrations are also a relatively common occurrence (Martin and Gordon, 1988; Bruland et al., 1991). This may result from rapid solubilization of iron from aerosol particles in the near-surface that is driven by photoreduction of iron in the sea, or on aerosol particles in the atmosphere (Zhuang et al., 1992).

The flux of iron produced by photoreduction appears to match the requirements of phytoplankton in the equatorial Pacific. We have estimated the biological requirements for iron from the Fe:C ratio of oceanic plankton (6×10^{-6} mol Fe:mol C; Morel et al., 1991), the doubling rate of plankton populations at 140°W on the equator (0.74 doublings d^{-1}; Chavez et al., 1991) and the standing stock of plankton carbon at 140°W (14 μg C l^{-1}; Chavez et al., 1991). These numbers give a requirement of 0.2 pmol Fe l^{-1} h^{-1}, slightly lower than the estimate of Rich and Morel (1990). The largest photoreduction rate calculated with the model in the upper 10 m is 25 pmol l^{-1} h^{-1} (Fig. 11), which is well in excess of the biological requirement. However, the average photoreduction rate determined over a 24 h cycle at light intensities from the surface to the 0.1% light level is only 2 pmol Fe l^{-1} h^{-1} (Fig. 11). This average rate is likely to just meet the population requirements since the plankton must compete with colloid formation reactions for the available iron. For comparison. Wells and Mayer (1991) have estimated the photoreduction rate in the equatorial Pacific at maximum light to be 0.7 pmol l^{-1} h^{-1}. This result differs significantly from our maximum rate because of the lower photoreduction rates of colloidal iron obtained in their work. These differences may
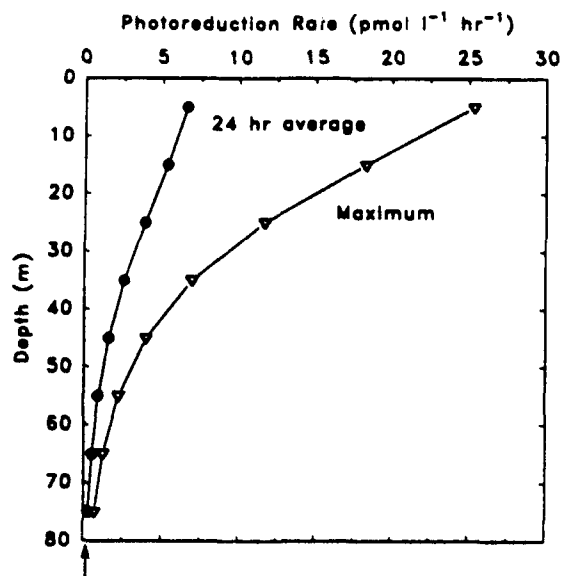
Fig. 11. Photoreduction rates vs. depth, assuming that the diffuse attenuation coefficient for light is 0.06 m⁻¹, corresponding to a 1% light level at 75 m, and that the initial, photolabile Fe concentration (dissolved + colloidal) was 0.15 nM. The maximum photoreduction rates occur in mid-morning, when the colloidal iron concentrations and light intensities are relatively high. The average photoreduction rates were calculated from the predicted photoreduction rates over a complete 24 h cycle. The arrow at 0.2 pmol l⁻¹ h⁻¹ shows the average iron requirement of the phytoplankton population calculated as discussed in the text.

arise because of the 100–1000-fold higher iron concentrations that they used in their work.

The thermal dissolution rate constant for iron colloids produced by oxidation of Fe(II) is 0.016 h⁻¹ in seawater containing EDTA (Rich and Morel, 1990). If colloidal iron concentrations average 0.1 nmol l⁻¹ in the euphotic zone of the equatorial Pacific, then the production rate of dissolved iron due to thermal dissolution might be 2 pmol l⁻¹ h⁻¹, very similar to the average photoreduction rate. However, the thermal dissolution rate of colloids in situ may be much lower than the rate measured in the laboratory if it is accelerated by the low Fe(III) concentrations that are maintained by the EDTA. If Fe(III) solubility is as low as suggested by the calculations of Motekaitis and Martell (1987), then thermal dissolution may not be a major contributor to the stock of biologically available iron.

The results of the incubation experiments demonstrated that all of the forms of iron that were added to seawater were made biologically available. However, aerosol particles appeared to stimulate the highest levels of growth despite the fact that the levels of TRFe were the lowest in this carboy. This effect was seen previously in equatorial Pacific waters by Martin et al. (1991). They found that 2–3 times more particulate organic carbon was produced with aerosols than with inorganic Fe(III) additions. The effect of aerosol iron may be due to the effects of other metals present in the particles (Arimoto et al., 1989). Coale (1991) found that manganese and copper also caused a small increase in growth in waters from the subarctic Pacific. Manganese alone did not increase chlorophyll levels or nitrate uptake in several incubation experiments performed on the FeLINE-I cruise. Martin et al. (1989) compared the effects of 10 nM Fe additions alone with the effects of a combined metal addition (10 nM Fe, 1 nM Mn and 0.1 nM Co) on phytoplankton chlorophyll production and nitrate uptake in samples from the subarctic Pacific. Phytoplankton doubling rates were highest in the treatments with the mixed metal additions at two of the three stations tested. These two stations were also the most iron limited, in the sense that they had the highest surface nitrate concentrations. Thus, it is reasonable to expect that aerosol particles containing iron would produce the highest growth.

The results of the modeling work suggest several constraints that can be placed on the occurrence of reduced Fe(II) in seawater. The model predicts maximum Fe(II) concentrations of only 1 × 10⁻⁴ nM when total reducible concentrations of iron are near 0.15 nM and the temperature is 25°C. Significant amounts of Fe(II) (> 10% of the dissolved iron) are possible only with large increases (≈ 100-fold) in both the rates of photoreduction and formation of FeC, or large decrease (≈ 30-fold) in the rate of Fe(II) oxidation. The rate of Fe(II) oxidation becomes 2 or 3 times slower than predicted as Fe(II) concentrations decrease (Waite and Morel, 1984; Millero et al., 1987). It has been suggested that these results may indicate the presence of Fe(II) binding ligands that reduce oxidation rates as the Fe(II) concentration

approached low nanomolar concentrations (Hudson et al., 1992). However, these small decreases in the Fe(II) oxidation rate might also be due to the loss of the radicals OH^-, O_2^- and H_2O_2 by pathways other than Fe(II) oxidation. Despite this, one should note that strong copper binding ligands exist at very low concentrations in seawater and these ligands can greatly reduce copper activity (Coale and Bruland, 1988). If similar ligands, which can bind Fe(II) or promote Fe(III) photoreduction, exist at sub-nanomolar concentrations, then they would not be detectable in the experiments discussed here and yet they would have an large impact at ambient iron concentrations. Large decreases in the iron oxidation rate also occur at low temperatures (Millero et al., 1987) and Fe(II) might become important at high latitudes.

Acknowledgements

References

Anderson, M.A. and Morel, F.M.M., 1982. The influence of aqueous iron chemistry on the uptake of iron by the coastal diatom *Thalassiosira weissflogii*. Limnol. Oceanogr., 27: 789–813.

Arimoto, R., Duce, R.A. and Ray, B.J., 1989. Concentrations, sources and air–sea exchange of trace elements in the atmosphere over the Pacific Ocean. In: J.P. Riley and R. Chester (Editors), Chemical Oceanography, 10. Academic, London, pp. 107–149.

Barber, R.T. and Chavez, F.P., 1991. Regulation of primary productivity rate in the equatorial Pacific. Limnol Oceanogr., 36: 1803–1815.

Bruland, K.W., Donat, J.R. and Hutchins, D.A., 1991. Interactive influences of bioactive trace metals on biological production in oceanic waters. Limnol. Oceanogr., 36: 1555–1577.

Byrne, R.H. and Kester, D.R., 1976. Solubility of hydrous ferric oxide and iron speciation in seawater. Mar. Chem., 4: 255–274.

Chavez, F.P., Buck, K.R., Coale, K.H., Martin, J.H., DiTullio, G.R., Welschmeyer, N.A., Jacobson, A.C. and Barber, R.T., 1991. Growth rates, grazing, sinking, and iron limitation of equatorial Pacific phytoplankton. Limnol. Oceanogr., 36: 1816–1833.

Coale, K.H., 1991. The effects of iron, manganese, copper and zinc on primary production and biomass in plankton of the subarctic Pacific. Limnol. Oceanogr., 36: 1851–1864.

Coale, K.H. and Bruland, K.W., 1988. Copper complexation in the Northeast Pacific. Limnol. Oceanogr., 33: 1084–1101.

Coale, K.H., Blain, S.P.G., Fitzwater, S.M., Coley, T.L. and Johnson, K.S., 1994. A mesoscale iron enrichment experiment: preliminary tests and experimental design. Deep-Sea Research, submitted.

Donaghey, P.L., Liss, P.S., Duce, R.A., Kester, D.R., Hanson, A.K., Villareal, T., Tindale, N. and Gifford, D.J., 1991. The role of episodic atmospheric nutrient inputs in the chemical and biological dynamics of oceanic ecosystems. Oceanography, 4: 62–70.

Duce, R.A. and Tindale, N.W., 1991. Atmospheric transport of iron and its deposition in the ocean. Limnol. Oceanogr., 36: 1715–1726.

Elrod, V., Johnson, K.S. and Coale, K.H., 1991. Determination of subnanomolar levels of iron(II) and total dissolved iron in seawater by flow injection analysis with chemiluminescence detection. Anal. Chem., 63: 893–898.

Finden, D.A.S., Tipping, E., Jaworski, G.H.M. and Reynolds, C.S., 1984. Light-induced reduction of natural iron(III) oxide and its relevance to phytoplankton. Nature, 309: 783–784.

Hanson, A.K., Tindale, N.W., Abdel-Moati, M.A.R., Cantu, A., O'Sullivan, D.W., Prentice, J.E., Warren, W.M., Fraher, J.R. and Kester, D.R., 1992. The influence of a rain event on iron, peroxide and phytoplankton in Equatorial Pacific surface waters. Trans. Am. Geophys. Union, 73: 82 (suppl.).

Hudson, R.J.M. and Morel, F.M.M., 1990. Iron transport in marine phytoplankton: kinetics of cellular and medium coordination reactions. Limnol. Oceanogr., 35: 1002–1020.

Hudson, R.J.M., Covault, D.T. and Morel, F.M.M., 1992. Investigations of iron coordination and redox reactions in seawater using ^{59}Fe radiometry and ion-pair solvent extraction of amphiphilic iron complexes. Mar. Chem., 38: 209–235.

Johnson. K.S., Willason, S.W., Wiesenburg, D.A., Lohrenz, S.E. and Arnone, R.A., 1989. Hydrogen peroxide in the Western Mediterranean Sea: a tracer for vertical advection. Deep-Sea Res., 36: 241–254.

Martin, J.H., 1992. Iron as a limiting factor in oceanic productivity. In: P. Falkowski and A.D. Woodhead (Editors), Primary Producity and Biogeochemical Cycles in the Sea. Plenum, New York, NY, pp. 123–127.

Martin, J.H. and Gordon, R.M., 1988. Northeast Pacific iron distributions in relation to phytoplankton productivity. Deep-Sea Res., 35: 177–196.

Martin, J.H., Gordon, R.M., Fitzwater, S. and Broenkow, W.W., 1989. VERTEX: phytoplankton/iron studies in the Gulf of Alaska. Deep-Sea Res., 36: 649–680.

Martin, J.H., Gordon, R.M. and Fitzwater, S.E., 1991. The case for iron. Limnol. Oceanogr., 36: 1793–1802.

Millero, F.J. and Sotolongo, S., 1989. The oxidation of Fe(II) with H_2O_2 in seawater. Geochim. Cosmochim. Acta, 53: 1867–1873.

Millero, F.J., Sotolongo, S. and Izaguirre, M., 1987. The oxidation kinetics of Fe(II) in seawater. Geochim. Cosmochim. Acta, 51: 793–801.

Moffett, J.W. and Zika, R.G., 1987. Reaction kinetics of hydrogen peroxide with copper and iron in seawater. Environ. Sci. Technol., 21: 804–810.

Mopper, K. and Zhou, Z., 1990. Hydroxyl radical photoproduction in the sea and its potential impact on marine processes. Science, 250: 661–664.

Morel, F.M.M., Hudson, R.J.M. and Price, N.M., 1991. Limitation of productivity by trace metals in the sea. Limnol. Oceanogr., 36: 1742–755.

Motekaitis, R.J. and Martell, A.E., 1987. Speciation of metals in the oceans.I. Inorganic complexes in seawater, and influence of added chelating agents. Mar. Chem., 21: 101–116.

Petasne, R.G. and Zika, R.G., 1987. Fate of superoxide in coastal sea water. Nature, 325: 516–518.

Plane, J.M.C., Zika, R.G., Zepp, R.G. and Burns, L.A., 1987. Photochemical modeling applied to natural waters. In: R.G. Zika and W.J. Cooper (Editors), Photochemistry of Environmental Aquatic Systems. Am. Chem. Soc., Washington, DC, Am. Chem. Soc. Symp. Ser., 327, pp. 250–267.

Reid, R.T., Live, D.H., Faulkner, D.J. and Butler, A., 1993. A siderophore from a marine bacterium with an exceptional ferric ion affinity constant. Nature, 366, 455–458.

Rich, H.W. and Morel, F.M.M., 1990. Availability of well-defined iron colloids to the marine diatom *Thalassiosira weisflogii*. Limnol. Oceanogr., 35: 652–662.

Strickland, J.D.H. and Parsons, T.R., 1972. A Practical Handbook of Seawater Analysis. Fish. Res. Board Can., Bull. 167, 2nd ed., 309 pp.

Stumm, W. and Morgan J.J., 1981. Aquatic Chemistry Wiley, New York, NY, 2nd ed., 780 pp.

Sunda, W.G., 1989. Trace metal interactions with marine phytoplankton. Biol. Oceanogr., 6, 411–442.

Sunda, W.G. and Huntsman, S.A., 1988. Effect of sunlight on redox cycles of manganese in the southwestern Sargasso Sea. Deep-Sea Res., 35: 1297–1317.

Trick, C.G., 1989. Hydroxamate-siderophore production and utilization by marine eubacteria. Curr. Microbiol., 18: 375–378.

Trick, C.G., Andersen, R.J., Gillam, A. and Harrison, P.J., 1983. Prorocentrum: an extracellular siderophore produced by the marine dinoflagellate *Prorocentrum minimum*. Science, 219: 306–308.

Waite, T.D. and Morel, F.M.M., 1984. Photoreductive dissolution of colloidal iron oxides in natural waters. Environ. Sci. Technol., 18: 860–868.

Wells, M.L., 1989. The availability of iron in seawater: a perspective. Biol. Oceanogr., 6: 463–476.

Wells, M.L. and Mayer, L.M., 1991. The photoconversion of colloidal iron oxyhydroxides in seawater. Deep-Sea Res., 38: 1379–1395.

Wells, M.L., Zorkin, N.G. and Lewis, A.G., 1983. The role of colloid chemistry in providing a source of iron to phytoplankton. J. Mar. Res., 41: 731–746.

Wells, M.L., Mayer, L.M. and Guillard, R.R.L., 1991a. A chemical method for estimating the availability of iron to phytoplankton in seawater. Mar. Chem., 33: 23–40.

Wells, M.L., Mayer, L.M., Donard, O.F.X., de Souza Sierra, M.M. and Ackelson, S.G., 1991b. The photolysis of colloidal iron in the oceans. Nature, 353: 248–250.

Zafiriou, O.C. and True, M.B., 1980. Interconversion of iron(III) hydroxy complexes in seawater. Mar. Chem., 8: 281–288.

Zhu, X., Prospero, J.M., Millero, F.J., Savoie, D.L. and Brass, G.W., 1992. The solubility of ferric ion in marine mineral aerosol solutions at ambient relative humidities. Mar. Chem., 38: 91–107.

Zhuang, G., Duce, R.A. and Brown, P.R., 1992. Link between iron and sulphur cycles suggested by detection of Fe(II) in marine aerosols. Nature, 355: 537–539.

Zika, R.G., Moffett, J.W., Petasne, R.G., Cooper, W.J. and Saltzman, E.S., 1985. Spatial and temporal variations of hydrogen peroxide in Gulf of Mexico waters. Geochim. Cosmochim. Acta, 49: 1173–1184.

Notes to Contributors

A detailed *Guide for Authors* is available upon request, and will also be printed in the first issue of each subscription year. You are kindly asked to consult this guide. Please pay special attention to the following notes:

Language
The official language of the journal is English.

Preparation of the text
(a) The manuscript should be typewritten with double spacing and wide margins and include at the beginning of the paper an abstract of not more than 500 words. Words to be printed in italics should be underlined. The metric system should be used throughout.
(b) The title page should include: the title, the name(s) of the author(s) and their affiliations.

References
(a) References in the text start with the name of the author(s), followed by the publication date in parentheses.
(b) The reference list should be in alphabetical order and on sheets separate from the text.

Tables
Tables should be compiled on separate sheets. A title should be provided for each table and they should be referred to in the text.

Illustrations
(a) All illustrations should be numbered consecutively and referred to in the text.
(b) Drawings should be completely annotated, the size of the lettering being appropriate to that of the drawings, but taking into account the possible need for reduction in size (preferably not more than 50%). The page format of *Marine Chemistry* should be considered in designing the drawings.
(c) Photographs must be of good quality, printed on glossy paper.
(d) Figure captions should be supplied on a separate sheet.

Proofs
One set of proofs will be sent to the author, to be checked for printer's errors. In the case of two or more authors please indicate to whom the proofs should be sent.

Reprints
Fifty reprints of each article published are supplied free of charge. Additional reprints can be ordered on a reprint order form, which will be sent to the first author upon acceptance of the article.

Submission of manuscripts
Three copies should be submitted to: Editorial Office *Marine Chemistry*, P.O. Box 1930, 1000 BX, Amsterdam, Netherlands. Illustrations should also be submitted in triplicate: one set should be in a form ready for reproduction; the other two may be of lower quality. Authors are requested to submit, with their manuscripts, the names and full addresses (plus fax numbers if possible) of four potential referees.

Submission of electronic text
In order to publish the paper as quickly as possible after acceptance, authors are encouraged to submit the final text also on a 3.5" or 5.25" diskette. Both double density (DD) and high density (HD) diskettes are acceptable. Make sure, however, that the diskettes are formatted according to their capacity (HD or DD) before copying the files onto them. Similar to the requirements for manuscript submission, main text, list of references, tables and figure legends should be stored in separate text files with clearly identifiable file names. The format of these files depends on the word processor used. Texts made with DisplayWrite, MultiMate, Microsoft Word, Samna Word, Sprint, Volkswriter, Wang PC, WordMARC, WordPerfect, Wordstar, or supplied in DCA/RTF, or DEC/DX format can be readily processed. In all other cases the preferred format is DOS text or ASC11. It is essential that the name and version of the wordprocessing program, type of computer on which the text was prepared, and format of the text files are clearly indicated. Authors are encouraged to ensure that the disk version and the hardcopy must be identical. Discrepancies can lead to proofs of the wrong version being made.

Submission of an article is understood to imply that the article is original and unpublished and is not being considered for publication elsewhere. Upon acceptance of an article by the journal, the author(s) will be asked to transfer the copyright of the article to the publisher. This transfer will ensure the widest possible dissemination of information.

Ocean Energies

Environmental, Economic and Technological Aspects of Alternative Power Sources

by R.H. Charlier and J.R. Justus

This timely volume provides a comprehensive review of current technology for all ocean energies. It opens with an analysis of ocean thermal energy conversion (OTEC), with and without the use of an intermediate fluid. The historical and economic background is reviewed, and the geographical areas in which this energy could be utilized are pinpointed. The production of hydrogen as a side product, and environmental consequences of OTEC plants are looked at. The competitiveness of OTEC with conventional sources of energy is analysed. Optimisation, current research and development potential are also examined.

Each chapter contains bibliographic references. The author has also distinguished between energy schemes which might be valuable in less-industrialized regions of the world, but uneconomical in the developed countries. A large number of illustrations support the text.

Every effort has been made to ensure that the book is readable and accessible for the specialist as well as the non-expert. It will be of particular interest to energy economists, engineers, geologists and oceanographers, and to environmentalists and environmental engineers.

Short Contents: .
1. State of the Art.
2. Offshore Wind Power Stations.
3. Ocean Current Energy Conversion.
4. Solar Ponds.
5. Waves.
6. Current Assessment of Ocean Thermal Energy Potential.
7. Is Tidal Power Coming of Age?
8. Salinity Energy.
9. Geothermal Energy.
10. Marine Biomass Energy.

Glossary. References and notes. Bibliography. Index

A complete list of contents is available from the publisher.

The Dutch Guilder (Dfl.) prices quoted apply worldwide. US $ prices quoted may be subject to exchange rate fluctuations. Customers in the European Community should add the appropriate VAT rate applicable in their country to the price.

ELSEVIER SCIENCE B.V.